

## Photo-CIDNP Reveals Differences in Compaction of Non-Native States of Lysozyme

Christian Schlörb, Sarah Mensch, Christian Richter, and Harald Schwalbe\*

*Institute for Organic Chemistry and Chemical Biology, Center for Biomolecular Magnetic Resonance,  
Johann Wolfgang Goethe-University, Marie-Curie-Strasse 11, D-60439 Frankfurt/M, Germany*

Received October 8, 2005; E-mail: schwalbe@nmr.uni-frankfurt.de

The structural investigation of non-native states of proteins is difficult due to their dynamic properties, but nuclear magnetic resonance (NMR) spectroscopy has played a key role in identifying long-range interactions for a number of non-native states of proteins (reviewed in<sup>1</sup>). The protein hen egg white lysozyme (HEWL) has been especially well characterized.<sup>2</sup> NMR studies revealed that clustering of hydrophobic residues occurs in HEWL even under strongly denaturing conditions and also in its reduced, cysteine-S-methylated and therefore disulfide-free forms (designated HEWL-S<sup>Me</sup> or WT-S<sup>Me</sup>) using a combination of NMR spectroscopy and site-directed mutagenesis.<sup>1</sup> Mutations in non-native HEWL-S<sup>Me</sup> result in major structural differences compared to wild-type (WT-S<sup>Me</sup>). Single-point mutations involving tryptophan induce significant changes in long-range interactions as inferred from <sup>15</sup>N R<sub>2</sub> relaxation rates and overall protein compactness as evidenced by a significant increase in the diffusion-derived hydrodynamic radius (*R<sub>h</sub>*) by 12% from WT-S<sup>Me</sup> to W62G-S<sup>Me</sup>.<sup>1</sup> Tryptophan residues therefore play a key role in stabilizing nonrandom conformational properties in WT-S<sup>Me</sup>.

Recently, we have developed an NMR method for the assignment of indole resonances in tryptophan side chains of non-native proteins.<sup>3</sup> This enables the investigation of structural and dynamical properties on the level of the tryptophan side chains, which are the key modulators of hydrophobic clustering and long-range interactions. In the same work, an HEWL variant, in which all cysteines have been replaced by alanines (designated all-Ala-HEWL), has been introduced. This mutant exhibits very similar properties as WT-S<sup>Me</sup> and therefore suits as a replacement for the S-methylated HEWL.

Here, we investigate the relaxation properties of the tryptophan side chains and the changes in solvent accessibility of tryptophan residues measured in a chemically induced dynamic nuclear polarization (CIDNP) experiment of wild-type and mutant lysozyme. Such additional information should be of importance for the experimental test of information derived from molecular dynamics simulations of non-native ensembles of proteins.<sup>4</sup> Photo-CIDNP NMR spectroscopy<sup>6</sup> can serve as a probe for the solvent accessibility of tryptophan side chains in all-Ala-HEWL and W62G-all-Ala-HEWL. We compare the CIDNP effect of all-Ala-HEWL and the mutant W62G-all-Ala-HEWL; the latter has been produced by site-directed mutagenesis from the all-Ala-HEWL gene.<sup>7</sup>

In the photo-CIDNP experiment, the relative solvent exposure of aromatic side chains can be probed by photochemically activated sensitizers such as flavins, which influence NMR peak intensities. Limited resolution of one-dimensional photo-CIDNP spectra has first been overcome by Lyon et al. with the development of a 2D-CIDNP experiment.<sup>8</sup> The larger CIDNP enhancement of <sup>15</sup>N compared to <sup>1</sup>H is exploited in the <sup>15</sup>N-<sup>1</sup>H 2D-CIDNP experiment, where the magnetization of <sup>15</sup>N nuclei is transferred in a single reverse INEPT step and detected on <sup>1</sup>H. Photoexcited flavin

mononucleotide (FMN) is used here to generate short-lived radical pairs with the tryptophan side chains, which finally leads to significant polarizations of the aromatic nuclei.

The 2D CIDNP spectra of the tryptophan indole region of both <sup>15</sup>N enriched all-Ala-HEWL (Figure 1b) and the W62G mutant thereof (Figure 1d) are compared to their respective standard <sup>1</sup>H,<sup>15</sup>N-HSQC spectra (Figure 1a and 1c).<sup>9</sup> The peak patterns of both the 2D <sup>15</sup>N-<sup>1</sup>H HSQC and the CIDNP spectrum of the tryptophan indole region of hen egg white lysozyme unfolded in 10 M urea<sup>8</sup> clearly look different from the respective spectra of all-Ala-HEWL. This might be due to the different temperature (318 K vs 303 K) and pH (3.6 vs 2.0) conditions as well as the presence of the denaturant. However, in both studies only five peaks are visible for the six tryptophans as two of the signals overlap.

The individual tryptophan indole peaks in the CIDNP spectra show a different intensity distribution than that in the HSQC spectra. The ratios of CIDNP versus HSQC peak intensities (Figure 2) are measures for the relative solvent accessibility of the various tryptophans as they reflect the degree of the polarization transfer from the FMN molecules. This is reported in Figure 2, where the highest CIDNP/HSQC ratio, resulting from the combined W28/W123 peak, is normalized to 1.0; the other ratios are scaled accordingly.

The ratio for W111 is only about half of the value for W28/W123, and the other tryptophan residues also exhibit significantly lower ratios. This coincides with their involvement in hydrophobic clustering and long-range interactions in non-native hen egg white lysozyme. The tryptophans involved in the most pronounced clusters are W62, W63 (designated cluster 3), and W111 (designated cluster 5) as judged by R<sub>2</sub> transverse relaxation analysis.<sup>1</sup> The structural findings from solvent accessibility information obtained by the two-dimensional photo-CIDNP studies therefore support the dynamical data from earlier works. The CIDNP/HSQC ratio distribution in the W62G mutant of all-Ala-HEWL is different from that of the all-Ala-HEWL: Only W111 shows a similar ratio, while the other ratios are significantly elevated, suggesting a similar solvent accessibility for all tryptophans in the W62G mutant but for W111. This is in accordance with mutational studies where it has been shown that the W62G mutation destroys most of the clustering in non-native lysozyme.<sup>1</sup>

In addition, the assignment of the tryptophan indole side chains in all-Ala-HEWL<sup>3</sup> permits the analysis of <sup>15</sup>N heteronuclear R<sub>2</sub> relaxation rates of the indole resonances in non-native lysozyme. These rates are recorded for all-Ala-HEWL and the W62G mutant and are shown in Table 1.<sup>10</sup> In agreement with the structural data from the photo-CIDNP experiments and the previously published analysis of the backbone relaxation rates,<sup>1</sup> the tryptophan residues W62 and W63 exhibit significantly elevated R<sub>2</sub> rates in all-Ala-HEWL in contrast to the W62G mutant, where the rates of all

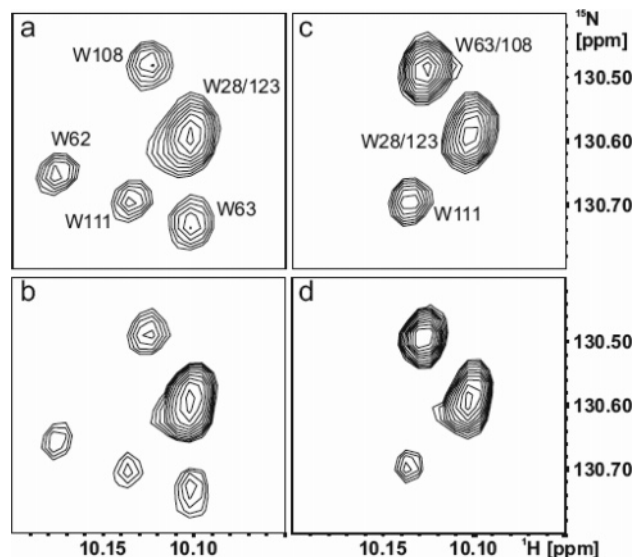


**Figure 1.** (a)  $^1\text{H}$ ,  $^{15}\text{N}$ -HSQC spectrum of the tryptophan side chain indole region of all-Ala-HEWL. (b) 2D-CIDNP spectrum of the same region. (c)  $^1\text{H}$ ,  $^{15}\text{N}$ -HSQC spectrum of the tryptophan side chain indole region of W62G-all-Ala-HEWL. (d) 2D-CIDNP spectrum of the same region.

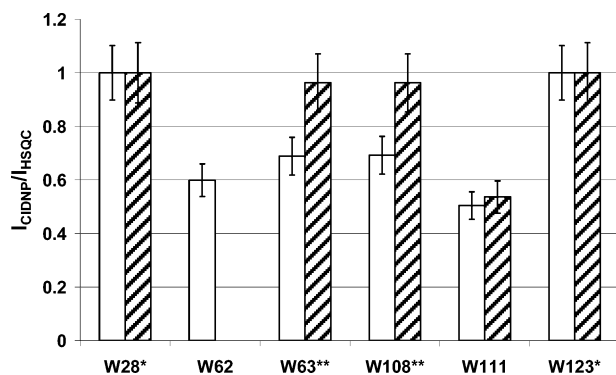


**Figure 2.** Comparison of the CIDNP/HSQC normalized intensity ratios of all-Ala-HEWL (open bars) and W62G-all-Ala-HEWL (dashed bars). (\*) The W28 and W123 peaks are coincident in all-Ala-HEWL and the W62G mutant. (\*\*) The W63 and W108 peaks are degenerated in W62G-all-Ala-HEWL. Peak intensities have been used for resolution purposes; however, integration of the resolved peaks yielded comparable results.

**Table 1.**  $^{15}\text{N}$   $R_2$  Relaxation Rates for Tryptophan Side Chain Indoles in all-Ala-HEWL and W62G-all-Ala-HEWL

	all-Ala-HEWL <sup>a</sup>	W62G-all-Ala-HEWL <sup>a</sup>
W28	2.3 ± 0.1	2.0 ± 0.1
W62	3.0 ± 0.1	
W63	3.1 ± 0.1	2.2 ± 0.1
W108	2.4 ± 0.1	2.2 ± 0.1
W111	2.6 ± 0.1	2.4 ± 0.1
W123	2.3 ± 0.1	2.0 ± 0.1

<sup>a</sup> All rates in Hz.

tryptophans are similar. These two tryptophans are involved in the most pronounced hydrophobic cluster in non-native lysozyme.

Interestingly, the W62G mutation neither influences the accessibility of W111 to FMN nor changes the relaxation properties of the backbone amide and side chain indole  $^{15}\text{N}$  nuclei. This indicates that the cluster around W111 does not interact with the other clusters, despite its sequential proximity to W108, and that either

these two tryptophans may be involved in two different clusters or the mutations disrupt interactions of only some of the participating side chains. The result of this study demonstrates the impact of the combination of 2D-CIDNP methods with the assignment of tryptophan side chains for structural studies of non-native states of proteins. The solvent exposure of tryptophan side chains is a valuable new parameter for the characterization of non-native ensembles of proteins and could in combination with molecular dynamics simulations provide a more precise view of the properties of such states. At the same time, molecular dynamics simulations will help answer the questions to what extent W111 and W108 are involved in a single or in multiple clusters.

**Acknowledgment.** This work was supported in part by the State of Hesse (BMRZ), the EU project UPMAN, and a stipend of the Fonds der Chemischen Industrie to C.S. The help of Boris Fürtig, Kai Schlepckow, and Karla Werner during the initial setup of the photo-CIDNP experiments is gratefully acknowledged.

## References

- (1) Klein-Seetharaman, J.; Oikawa, M.; Grimshaw, S. B.; Wirmer, J.; Duchardt, E.; Ueda, T.; Imoto, T.; Smith, L. J.; Dobson, C. M.; Schwalbe, H. *Science* **2002**, *295*, 1719–1722. Wirmer, J.; Schlörb, C.; Klein-Seetharaman, J.; Hirano, R.; Ueda, T.; Imoto, T.; Schwalbe, H. *Angew Chem Int Ed Engl.* **2004**, *43*, 5780–5785.
- (2) Schwalbe, H.; Fiebig, K. M.; Buck, M.; Jones, J. A.; Grimshaw, S. B.; Spencer, A.; Glaser, S. J.; Smith, L. J.; Dobson, C. M. *Biochemistry* **1997**, *36*, 8977–8991.
- (3) Schlörb, C.; Ackermann, K.; Richter, C.; Wirmer, J.; Schwalbe, H. *J. Biomol. NMR* **2005**, *33*, 95–104.
- (4) Quantification of solvent accessibility can be accomplished by time-resolved CIDNP; however, a semiquantitative analysis can also be performed with the data presented here, as discussed in ref 5.
- (5) Morozova, O. B.; Yurkovskaya, A. V.; Sagdeev, R. Z.; Mok, K. H.; Hore, P. J. *J. Phys. Chem. B* **2004**, *108*, 15355–15363.
- (6) Kaptein, R. In *NMR Spectroscopy in Molecular Biology*; Pullman, B., Ed.; D. Reidel: Dordrecht, 1978; pp 211–229. Kaptein, R. *Biol. Magn. Reson.* **1982**, *4*, 145–191. Kaptein, R.; Dijkstra, K.; Nicolay, K. *Nature* **1978**, *274*, 293–294. Hore, P. J.; Broadhurst, R. W. *Prog. Nucl. Magn. Reson. Spectrosc.* **1993**, *25*, 345–402.
- (7) All-Ala-HEWL and W62G-all-Ala-HEWL have been expressed and purified as described before.<sup>3</sup> The gene coding for W62G-all-Ala-HEWL has been generated by site-directed single-point mutation of the All-Ala-HEWL gene using the QuikChange Site-Directed Mutagenesis Kit (Stratagene, La Jolla, CA) and appropriate forward and backward primers.
- (8) Lyon, C. E.; Jones, J. A.; Redfield, C.; Dobson, C. M.; Hore, P. J. *J. Am. Chem. Soc.* **1999**, *121*, 6505–6506.
- (9) The 2D-photo-CIDNP and the conventional  $^1\text{H}$ ,  $^{15}\text{N}$  HSQC spectra have been recorded on a 700 MHz spectrometer equipped with a 5 mm  $^1\text{H}$ ,  $^{13}\text{C}$ ,  $^{15}\text{N}$  cryogenic probe with z-axis gradients at a temperature of 303 K. The NMR samples contained 200  $\mu\text{M}$  All-Ala-HEWL or W62G-all-Ala-HEWL, respectively, 200  $\mu\text{M}$  FMN, and 10%  $\text{D}_2\text{O}$ ; the pH was adjusted to 2.0. A CW argon ion laser emitting at 488/515 nm has been used as a light source in a setup as described before. The output power of the laser has been adjusted to 500 mW for the CIDNP experiments. Both  $^1\text{H}$ - $^{15}\text{N}$ -HSQC and  $^{15}\text{N}$ - $^1\text{H}$ -photo-CIDNP spectra have been recorded with 2 scans and 64 increments in the indirect dimension at sweep widths of 9766 Hz ( $^1\text{H}$ ) and 355 Hz ( $^{15}\text{N}$ ), respectively. The two-dimensional photo-CIDNP experiments have been performed using a pulse sequence as described<sup>8</sup> with 50 ms laser pulses. The CIDNP/HSQC intensity ratios have been calculated for every peak, and the highest value has been normalized to 1.0. Errors for the peak intensities have been extracted from the signal-to-noise ratio; the error bars for the CIDNP/HSQC ratios have been calculated by error propagation from the intensity errors.
- (10) The heteronuclear  $^{15}\text{N}$   $R_2$  relaxation investigations have been carried out on a 600 MHz spectrometer equipped with a 5 mm  $^1\text{H}$ ,  $^{13}\text{C}$ ,  $^{15}\text{N}$  pulsed-field z-gradient probe. NMR samples contained 500  $\mu\text{M}$  protein and 10%  $\text{D}_2\text{O}$  in deionized water with the pH value adjusted to 2.0. Heteronuclear  $^{15}\text{N}$   $R_2$  relaxation rates have been obtained by fitting peak intensities measured as a function of relaxation delay (ranging from 17.1 to 307.2 ms) using a pseudo-3D variant of the standard Bruker pulse sequence at a temperature of 293 K to a single-exponential decay. A two-parameter single-exponential decay function has been used for the fitting with SigmaPlot (Systat Software Inc.). Errors for the relaxation rates have been extracted from the fits.

JA056757D